

## ORIGINAL ARTICLE

## Synthesis and Characterization of LaF<sub>3</sub>:Ce Scintillator Material

E. Sukirman<sup>1,\*</sup>, Y. Purwamargapratala<sup>2</sup>, B. Sugeng<sup>1</sup>, Wahyudianingsih<sup>1</sup>, I. Gunawan<sup>1</sup>, S. Ahda<sup>3</sup>, A. Sudjatno<sup>1</sup> and A. Dimiyati<sup>1</sup>

<sup>1</sup>Research Center for Radiation Detection and Nuclear Analysis Technology, Research Organization for Nuclear Energy, National Research and Innovation Agency, KST BJ Habibie, Jalan Raya Puspiptek, Tangerang Selatan 15314, Banten, Indonesia.

<sup>2</sup>Research Center for Advanced Material, Research Organization for Nanotechnology and Materials, National Research and Innovation Agency, KST BJ Habibie, Jalan Raya Puspiptek, Tangerang Selatan 15314, Banten, Indonesia.

<sup>3</sup>Research Center for Nuclear Reactor Technology, Research Organization for Nuclear Energy, National Research and Innovation Agency, KST BJ Habibie, Jalan Raya Puspiptek, Tangerang Selatan 15314, Banten, Indonesia.

**ABSTRACT** – Synthesis and characterization of the LaF<sub>3</sub>:Ce scintillator have been carried out. Synthesis was carried out using the co-precipitation method. In this study, the raw materials used were NaF, LaCl<sub>3</sub>·7H<sub>2</sub>O, and Ce(NO<sub>3</sub>)<sub>3</sub>·6H<sub>2</sub>O with ethanol and distilled water as a solvent, while the surfactants used were oleic acid. In this study, the compound LaF<sub>3</sub>:0.2Ce was synthesized. The sample was characterized using an X-Ray Diffractometer (XRD), a Scanning Electron Microscope (SEM), and a Spectrofluorometer. The analyzed data showed that the 82.6 weight fraction of the LaF<sub>3</sub>:0.2Ce phase has precipitated, accompanied by the formation of NaCl and C<sub>2</sub>Ce phases of 5.1 and 12.3 weight fraction, respectively. The NaCl phase is a by-product of the chemical reaction:  $x\text{LaCl}_3 \cdot 7\text{H}_2\text{O} + z\text{CeCl}_3 \cdot 7\text{H}_2\text{O} + 3\text{NaF} \rightarrow \text{La}_x\text{Ce}_z\text{F}_3 + 3\text{NaCl} + 7\text{H}_2\text{O}$  which could be removed from the precipitate solution by an appropriate separation method, while the C<sub>2</sub>Ce one appeared as a result of heating the sample at 400°C. The LaF<sub>3</sub>:Ce scintillator sample shows the phenomenon of a bluish glow with a lifetime,  $t = 6 \times 10^{-10}$  seconds, even in the presence of a foreign phase. The existence of NaCl and C<sub>2</sub>Ce as a local environment still makes LaF<sub>3</sub>:0.2Ce has normal lifetime characteristics.

**ARTICLE HISTORY**

Received: 9 February 2023

Revised: 2 April 2023

Accepted: 4 April 2023

**KEYWORDS**

Scintillator materials

LaF<sub>3</sub>:Ce

Co-precipitation

### INTRODUCTION

The detection of gamma-ray emissions from radionuclides hidden in a container is an essential issue for national security. Usually, today's gamma-ray scintillator detectors use single crystals of Tl-doped NaI [1]. The NaI:Tl single crystal scintillator is currently the most efficient single crystal [2]. However, the use of high-quality NaI:Tl crystals limits the functionality of these detectors due to cost, hygroscopicity, limited choice of compositions, and frequent defects during growth [3]. Therefore, it is necessary to develop synthetic materials that are more durable, easier to produce with flexible sizes, and more cost-effective in production.

An alternative method for making scintillation detectors is by compositing nanoscale phosphor powder (nanophosphors) into a transparent polymer matrix, resulting in transparent nanophosphors. Thus, large nanocomposite detectors can be fabricated. Nanophosphors can be defined as nanoparticles of transparent dielectrics (hosts) doped with optically active ions (activators) so that the emission of light happens due to the electronic transitions between the levels of the impurity ions inside the bandgap of the host (characteristic luminescence) [4]. Nanophosphor powder encapsulated in a polymer matrix can provide better scintillation performance. Because this scintillator has the potential to be environmentally insensitive, mechanically durable, and flexible, both in terms of size and geometry, this nanophosphor, after being encapsulated in a polymer matrix, can provide increased performance for various applications, such as for portal monitors [5].

The growing interest in scintillator detectors that utilize nanophosphor has led to the emergence of the cerium-doped lanthanum trifluoride, LaF<sub>3</sub>:Ce. Some researchers have focused on the development of LaF<sub>3</sub> nanocrystals doped with rare earth ions due to their high photochemical stability, low toxicity, and biocompatibility [6]. Over the past few decades, many studies have been made on the synthesis and characterization of Ce-doped LaF<sub>3</sub> nanoparticles. Many techniques have been used to synthesize lanthanide-based nanocrystals. In previous research [7], cerium-doped LaF<sub>3</sub> nanoparticles (LaF<sub>3</sub>:Ce NPs) were successfully synthesized using hydrothermal reaction [7]. In other papers, cerium and alanine-doped LaF<sub>3</sub> nanocrystals have been synthesized from water-soluble chlorides in distilled water and then dried in a microwave oven to reduce agglomeration [8]. Cerium ions doped lanthanum fluoride (LaF<sub>3</sub>:Ce) nanopowder was synthesized using an irradiation technique with high-intensity ultrasound [9]. LaF<sub>3</sub> was synthesized using LaCl<sub>3</sub> and NH<sub>4</sub>F as starting materials in deionized water as a solvent via a microwave-assisted technique [10]. The LaF<sub>3</sub>:Ce water-soluble nanoparticles have been synthesized by wet chemical method with subsequent irradiation by microwaves to reduce agglomeration [11]. In a previous study [12], LaF<sub>3</sub> nanocrystals were doped with 0–10% Ce. In this study, distilled water and methanol were used as solvents, and DI-chitosan as a deagglomeration to form a transparent colloidal solution. All the experiments mentioned above have successfully produced a single phase of the LaF<sub>3</sub>:Ce scintillator. In the present experiment, the synthesis of LaF<sub>3</sub>:Ce was carried out using the co-precipitation method using distilled water, ethanol as

solvents, and oleic acid as surfactants. The aim is to explore a little further into a synthesis process using the chemical co-precipitation method and characterization of a sample of the LaF<sub>3</sub>: Ce scintillator nanoparticles in case of the presence of other phases.

## EXPERIMENTAL METHOD

### Materials and Instruments

Synthesis of cerium-doped lanthanum fluoride (LaF<sub>3</sub>) nanoparticles was carried out using a simple and affordable method. The raw materials used were NaF (0.1MF<sup>-</sup>, analytical standard, Sigma-Aldrich), LaCl<sub>3</sub>•7H<sub>2</sub>O (ACS reagent, Sigma Aldrich), Ce(NO<sub>3</sub>)<sub>3</sub>•6H<sub>2</sub>O (99% trace metal base, Aldrich), oleic acid, ethanol, and DIW (deionization water, distilled water). The equipment includes an analytical balance for weighing raw materials, a hot plate accompanied by a magnetic stirrer, a glass beaker to precipitate the precursor, a filter device, and an oven for precursor drying.

### Method and Procedure

The nonstoichiometric phase La<sub>1-y</sub>Ce<sub>y</sub>F<sub>3</sub> (y = 0.20) with a tysonite (LaF<sub>3</sub>) structure has been prepared by the co-precipitation method. In this study, 3.0 g of La<sub>0.8</sub>Ce<sub>0.2</sub>F<sub>3</sub>, which is then written LaF<sub>3</sub>:0.2Ce, was synthesized. In the first step, 458.9 ml (1.927 g) 0.1 M NaF was dissolved in a beaker glass containing 70 ml DIW. Then 7.2 grams of oleic acid was added, dispersed in 50 ml of absolute ethanol. The resulting solution was stirred using a magnetic stirrer with a bar magnet rotation rate of 300 rpm while heated at 78° C for 2 hours. To this solution was added a solution of 4.544 g LaCl<sub>3</sub>•7H<sub>2</sub>O and 1.328 g Ce(NO<sub>3</sub>)<sub>3</sub>•6H<sub>2</sub>O in 40 ml DIW. The amount of Ce(NO<sub>3</sub>)<sub>3</sub>•6H<sub>2</sub>O added is 20% Ce because, based on the experimental results of Rogers et al. [13], the composition of 20% Ce is optimum.

The solution containing the precipitate was then cooled to room temperature, filtered, and washed using ethanol in water with a ratio of 1:1. Besides that, the removal of impurities was also carried out with an ultrasonic cleaner. After decantation, a gel-shaped solid was obtained. Then the gel was dried in an oven at 110°C for 24 hours, followed by annealing at 400°C/2 hours. The morphology and chemical elements of the sample were observed with scanning electron microscope (SEM)/energy dispersive spectroscopy (EDS), JSM 6510 LA JEOL Type at room temperature. The X-ray diffraction data were collected in the scattering angular range of 10°–80° in the interval of 0.02° at room temperature measurements using X-Ray Diffraction (XRD) of Malvern PaNalytical Empeyrean type. X-ray diffraction data were analyzed with the Rietveld method using the HighScore software. The fluorescence (luminescence) characteristics of the sample, namely the excitation spectrum, emission spectrum, and lifetime of the luminescent material, were identified with a Spectrofluorometer, Horiba FluoroMax PLUS.

Fluorescence emission spectra are obtained when the excitation wavelength is set, and the emission wavelength is scanned to obtain a plot of intensity versus emission wavelength. The fluorescence excitation spectrum was obtained when the emission wavelength was set, and the excitation wavelength was scanned. The fluorescence lifetime of a molecule is the average period of time it spends in an excited state. This lifetime depends on the type of molecule and the local environment. Usually, excited states decay exponentially, and the intensity decay as a function of time is given by equation (1):

$$I(t) = I_0 \exp(-t/\tau) \quad (1)$$

where I(t) is the intensity at time t, I<sub>0</sub> is the normalization term (pre-exponential factor), and τ is the fluorescence lifetime or the time required for the emission intensity to decay to 1/e of its initial value [14].

## RESULT AND DISCUSSION

After the gel precursor was dried in the oven at 110°C for 24 hours, the sample remained in the form of a very sticky gel. This means the oleic acid has not been lost and is still mixed with the sample. This oleic acid, at room temperature, is a viscous liquid with a pale yellow or brownish-yellow color. This acid has a distinctive aroma, is insoluble in water, and has a boiling point of 360°C. Therefore, the sample was heated again at 400°C so the oleic acid was lost from burning. After burning, a dry white LaF<sub>3</sub>:0.2Ce bulk sample was produced, so grinding was done to obtain a fine powder.

Scanning electron microscope (SEM) micrograph of the sample is shown in Figure 1, which displays the shape of elongated crystal grains with heterogeneous sizes ranging from 1–50 μm. The identification of the elements in the sample was carried out using the Energy Dispersive Spectroscopy (EDS) at the A, B, and C sites, while C represented the elements in the green box in Figure 1, and the EDS spectrums were shown in Figure 2, Figure 3, and Figure 4 for A, B, and C sites, respectively. The chemical elements present at the A, B, and C sites are shown in Table 1, Table 2, and Table 3, respectively. The content of those chemical elements was calculated by the ZAF method that has been installed on the SEM tool system in a semi-quantitative manner. ZAF method means a correction that takes into account the following three effects on the characteristic X-ray intensity when performing quantitative analysis: 1) atomic number (Z) effect, 2) absorption (A) effect, and 3) fluorescence excitation (F) effect.

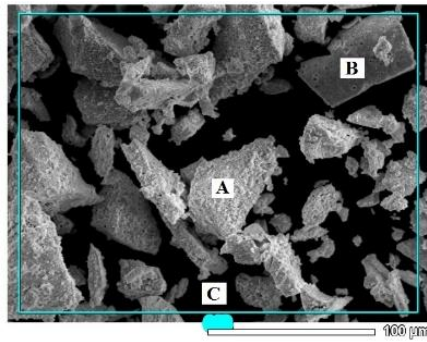


**Figure 1.** SEM image of LaF<sub>3</sub>:0.2Ce sample

From the EDS spectrum, it can be seen that the sample is arranged in addition to La, F, and Ce as expected; there are also Na, Cl, and C atoms. It is suspected that other than LaF<sub>3</sub>:0.2Ce, there may also be a NaCl phase as a by-product of the reaction based on the reaction equation:  $x\text{LaCl}_3 \cdot 7\text{H}_2\text{O} + z\text{CeCl}_3 \cdot 7\text{H}_2\text{O} + 3\text{NaF} \rightarrow \text{La}_x\text{Ce}_z\text{F}_3 + 3\text{NaCl} + 7\text{H}_2\text{O}$ . The presence of C atoms in the sample results from the sample being heated at 400°C to remove the oleic acid, which leaves the carbon.

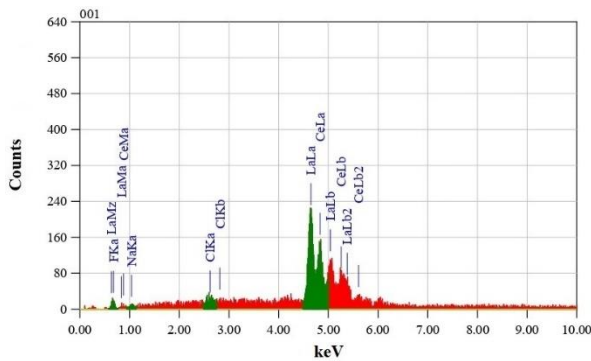


**Figure 2.** EDS spectrum of LaF<sub>3</sub>:0.2Ce sample at A site

**Table 1.** Excitation energy (keV), mass (%), error (%), and atom (%) of the elements at A site determined by the ZAF method with a fitting coefficient: 0.4824

| Element      | Energy (keV) | Mass (%)      | Error (%) | Atom (%)      |
|--------------|--------------|---------------|-----------|---------------|
| F K*         | 0.677        | 0.75          | 0.13      | 5.02          |
| Na K*        | 1.041        | 0.70          | 0.20      | 3.88          |
| Cl K*        | 2.621        | 0.49          | 0.09      | 1.76          |
| La L         | 4.648        | 50.35         | 0.40      | 46.07         |
| Ce L         | 4.837        | 47.71         | 0.55      | 43.28         |
| <b>Total</b> |              | <b>100.00</b> |           | <b>100.00</b> |

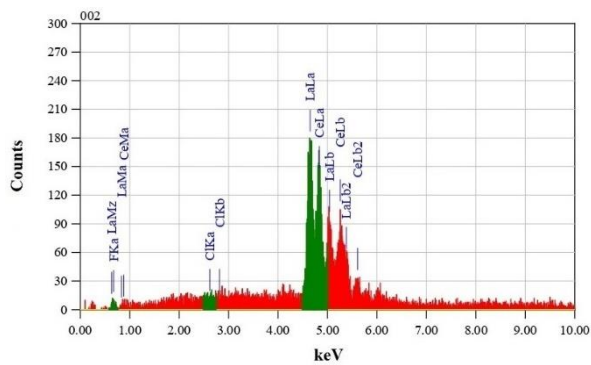


**Figure 3.** EDS spectrum of LaF<sub>3</sub>:0.2Ce sample at B site

**Table 2.** Excitation energy (keV), mass (%), error (%), and atom (%) of the elements at A site determined by the ZAF method with a fitting coefficient: 0.5480

| Element      | Energy (keV) | Mass (%)      | Error (%) | Atom (%)      |
|--------------|--------------|---------------|-----------|---------------|
| F K*         | 0.677        | 0.12          | 0.16      | 0.88          |
| Cl K*        | 2.621        | 0.18          | 0.11      | 0.70          |
| La L         | 4.648        | 44.52         | 0.48      | 44.16         |
| Ce L         | 4.837        | 55.18         | 0.65      | 54.26         |
| <b>Total</b> |              | <b>100.00</b> |           | <b>100.00</b> |

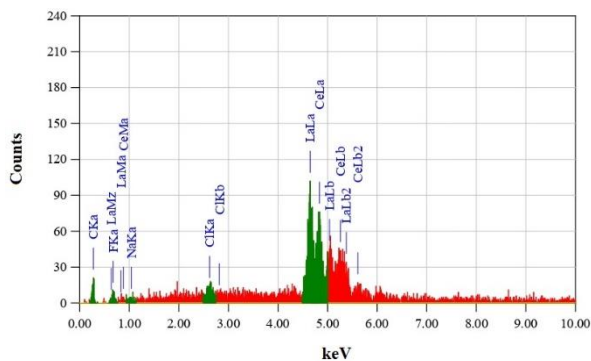


**Figure 4.** EDS spectrum of LaF<sub>3</sub>:0.2Ce sample at C site

**Table 3.** Excitation energy (keV), mass (%), error (%), and atom (%) of the elements at A site determined by the ZAF method with a fitting coefficient: 0.5582

| Element      | Energy (keV) | Mass (%)      | Error (%) | Atom (%)      |
|--------------|--------------|---------------|-----------|---------------|
| C K*         | 0.277        | 6.95          | 0.07      | 44.12         |
| F K*         | 0.677        | 0.75          | 0.15      | 3.01          |
| Na K*        | 1.041        | 0.24          | 0.21      | 0.79          |
| Cl K         | 2.621        | 1.13          | 0.10      | 2.42          |
| La L         | 4.648        | 42.22         | 0.42      | 23.17         |
| Ce L         | 4.837        | 48.71         | 0.58      | 26.50         |
| <b>Total</b> |              | <b>100.00</b> |           | <b>100.00</b> |

The X-ray diffraction pattern from the  $\text{LaF}_3:0.2\text{Ce}$  sample was analyzed with the help of the Rietveld method using the High Score software. The result is shown in Figure 5, which is the superposition diffraction pattern of the three phases, namely  $\text{La}_{0.8}\text{Ce}_{0.2}\text{F}_3$ ,  $\text{NaCl}$ , and  $\text{C}_2\text{Ce}$ , as predicted. Table 4 shows the crystal structure parameters of  $\text{La}_{0.8}\text{Ce}_{0.2}\text{F}_3$  space group:  $\text{P6}_3/\text{mmc}$ , No. 194,  $\alpha = \beta = 90^\circ$ ,  $\gamma = 120^\circ$ , lattice parameters:  $a = b = 4.1393(1) \text{ \AA}$ ,  $c = 7.3220(3) \text{ \AA}$ ,  $V = 108.8 \text{ \AA}^3$ , weight fraction: 82.6 %. This data is in good agreement with the hexagonal phase structure known from the Crystallography Open Database, cif file no. 1538557 [15] and in accordance with the research result by K. Schlyter [16]. Table 5 shows the crystal structure parameters of  $\text{NaCl}$ , space group:  $\text{Fm}\text{-}3\text{m}$ , No. 225,  $\alpha = \beta = \gamma = 90^\circ$ , lattice parameters:  $a = b = c = 5.632(1) \text{ \AA}$ ,  $V = 178.6 \text{ \AA}^3$ , weight fraction: 5.1 %, in accordance with the Crystallography Open Database, cif file no. 1000041 [17]. Table 6 shows the crystal structure parameters of  $\text{C}_2\text{Ce}$ , space group:  $\text{I4}/\text{mmm}$ , No. 139,  $\alpha = \beta = \gamma = 90^\circ$ , lattice parameters:  $a = b = 3.893(5) \text{ \AA}$ ,  $c = 5.63(1) \text{ \AA}$ ,  $V = 85.4 \text{ \AA}^3$ , weight fraction: 12.3 %, in accordance with the Crystallography Open Database, cif file no. 1528322 [18].

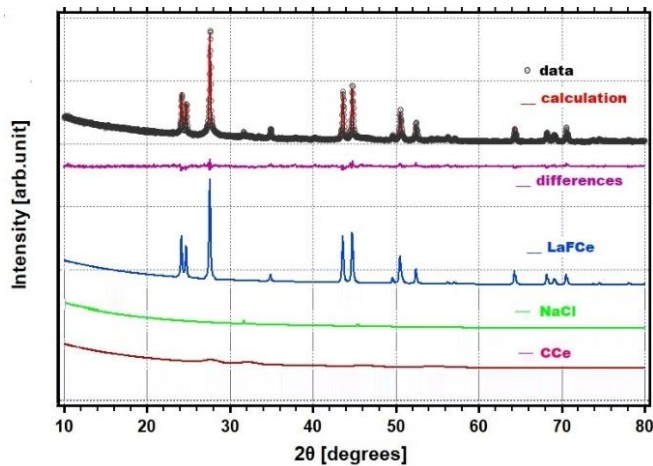


Figure 5. The X-ray diffraction pattern analyzed using the Rietveld method from  $\text{LaF}_3:0.2\text{Ce}$  sample

Table 4. Crystal structure parameters of  $\text{La}_{0.8}\text{Ce}_{0.2}\text{F}_3$

| Atom | $g_j$ | $x_j$ | $y_j$  | $z_j$    |
|------|-------|-------|--------|----------|
| Ce   | 0.5   | 0.333 | 0.6670 | 0.250    |
| F(1) | 1.0   | 0.000 | 0.000  | 0.250    |
| La   | 0.5   | 0.333 | 0.6670 | 0.250    |
| F(2) | 1.0   | 0.333 | 0.6670 | 0.579(1) |

Table 5. Crystal structure parameters of  $\text{NaCl}$

| Atom | $g_j$ | $x_j$ | $y_j$ | $z_j$ |
|------|-------|-------|-------|-------|
| Na   | 1.0   | 0.0   | 0.0   | 0.0   |
| Cl   | 1.0   | 0.5   | 0.5   | 0.5   |

Table 6. Crystal structure parameters of  $\text{C}_2\text{Ce}$

| Atom | $g_j$ | $x_j$ | $y_j$ | $z_j$ |
|------|-------|-------|-------|-------|
| C    | 1.0   | 0.0   | 0.0   | 0.349 |
| Ce   | 1.0   | 0.0   | 0.0   | 0.0   |

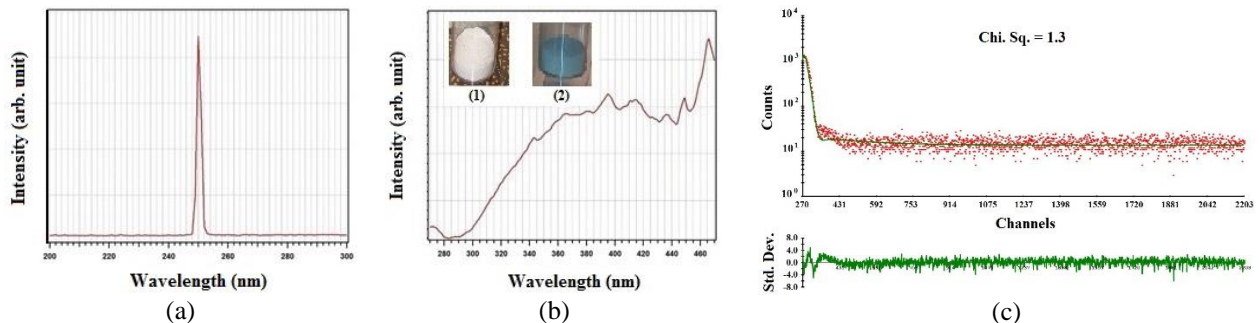


Figure 6. (a) Excitation spectrum for  $\text{Ce}^{3+}$  taken in one band centered at 250 nm, (b) emission spectrum in the wavelength range 270 nm ~ 470 nm, (c) and decay curve of photon emission

Figure 5 shows that the calculated intensity (solid line) almost completely coincides with the observed intensity (dotted line). This means the sample consists of three phases, namely  $\text{La}_{0.8}\text{Ce}_{0.2}\text{F}_3$ ,  $\text{NaCl}$ , and  $\text{C}_2\text{Ce}$ . No other phase was detected besides the three phases. In addition, as far as the accuracy of the instrument was concerned, there was a compound containing Ce observed, namely  $\text{C}_2\text{Ce}$ . Not all 20%Ce added to the precursor goes into the  $\text{LaF}_3$  host lattice. This most likely happened when the  $\text{LaF}_3:0.2\text{Ce}$  sample was heated at  $400^\circ\text{C}$ ; there is Ce that does not enter the host lattice and reacts with C to form  $\text{Ce}_2\text{C}$ . Fitting quality is expressed by parameter  $\chi^2$ , where the smaller the value of this parameter is close to 1.0, the better the fitting quality; for this experiment  $\chi^2 = 1.4$ .

The average crystallite size has been calculated from the line broadening of the highest XRD peak using Debye Scherrer formula given by:  $D = k\lambda/\beta \cos\theta$ , where  $D$  is the average crystallite size (in  $\text{\AA}$ ),  $k$  is the shape factor which is often assigned a value of 0.89,  $\lambda$  is the wavelength of  $\text{CuK}\alpha$  radiation (equal to  $1.5418 \text{ \AA}$ ),  $\beta$  is the full width at half maximum and  $\theta$  is the Bragg's angle [19]. Taking into consideration the correction due to instrumental broadening ( $0.01^\circ$ ), and based on the highest diffraction peak,  $2\theta_{(101)}=27.553^\circ$ , obtained  $D = 52 \text{ \AA}$ . Thus the  $\text{LaF}_3:0.2\text{Ce}$  is a nanocrystalline material because it meets the criteria that a material is considered nanocrystalline if it has a crystallite size smaller than 100 nm.

As shown in Figure 6 (a), the excitation spectrum for  $\text{Ce}^{3+}$  is taken in a band centered at 250 nm, and an emission spectrum is produced in the wavelength range of 270 nm ~ 470 nm, as shown in Figure 6 (b). The emission spectrum consists of a wide band from 270 to 470 nm with a maximum of 465 nm, and there are five sharp peaks centered at 342,

395, 415, 435, and 450 nm. Concerning the wavelength data of visible light (Table 7), it appears that in the wavelength range of 400–450 nm, LaF<sub>3</sub>:0.2Ce samples emit violet light. In the 450–500 nm range, LaF<sub>3</sub>:0.2Ce emits a blue light emission spectrum. Therefore, the sample of LaF<sub>3</sub>:0.2Ce powder has a bluish color, as shown in the insert of Figure 6 (b)(2), whereas, before exposure to violet light, the LaF<sub>3</sub>:0.2Ce sample looks white, as shown in the insert in Figure 6 (b)(1). After excitation, the molecule remains in the excited state for a short time before returning to the ground state. The time that a molecule is in an excited state is called its lifetime. The fluorophore lifetime can range from nanoseconds (10<sup>-9</sup> seconds) to picoseconds (10<sup>-12</sup> seconds) [20]. In this study, the lifetime of LaF<sub>3</sub>:0.2Ce sample is  $\tau = 6 \times 10^{-10}$  seconds obtained from the decay curve of photon emission in Figure 6 (c). As mentioned above, the lifetime depends on the local environment, but in this case, the existence of NaCl and C<sub>2</sub>Ce as a local environment still makes LaF<sub>3</sub>:0.2Ce has normal lifetime characteristics.

**Table 7.** The color and wavelength of visible light [21]

| Color             | Wavelength (nm) |
|-------------------|-----------------|
| mid-Ultraviolet   | 190–320         |
| near-UV           | 320–400         |
| Violet and Indigo | 400–450         |
| Blue and Aqua     | 450–500         |
| Green             | 500–570         |
| Yellow and Orange | 570–610         |
| Red               | 610–750         |
| near-IR           | 750–2.500       |

The best luminous material currently is single crystal NaI(Tl). This luminous material produces photon emission with an intensity of almost two to three orders higher than the composite nanophosphor scintillator [22]. One way to increase the photon emission intensity of the LaF<sub>3</sub>:Ce luminescent material is by (1) increasing the percentage of nanophosphors in the polymer matrix so that the number of luminescent sites increases in proportion to the number of luminescent sites on the single crystal, which on single crystals of NaI(Tl) composed entirely of luminous sites; (2) the composite nanophosphor scintillator must be single-phase so that all parts in the material are luminescence centers.

The La<sup>3+</sup> ion is the only rare earth element that is not used immediately; the reason stems from the fact that the La<sup>3+</sup> is not optically active because it has a completely filled frontier-4f orbital. However, the advantage of using an inorganic matrix La<sup>3+</sup> (hexagonal LaF<sub>3</sub>) is that this material has a flexible structure. This is a key factor that allows in the synthesis, various types of dopants can be easily incorporated into the lattice points of La<sup>3+</sup> ions. In rare earth (RE)-doped La<sup>3+</sup> matrix materials, the optical properties of the material become highly dependent on the type of dopants, and the optical performance can be adapted to convert via a multi-photon process from high-energy photons (UV, X-rays, and Gamma rays) and low-energy photons (near-infrared-NIR) to produce light in the visible region [23].

## CONCLUSION

The synthesis using the chemical precipitation method succeeded in precipitating the compound LaF<sub>3</sub>:0.2Ce as seen from the x-ray diffraction data, which displayed sharp diffraction peaks even though accompanied by the formation of the NaCl and C<sub>2</sub>Ce phases. The first-mentioned phase could be removed from the precipitate solution by an appropriate separation method, while the second-mentioned one appeared as a result of heating the sample at 400°C. Synthesis using the chemical precipitation method has also succeeded in showing the phenomenon of a bluish glow. The existence of NaCl and C<sub>2</sub>Ce as a local environment still makes LaF<sub>3</sub>:0.2Ce have normal lifetime characteristics.

## ACKNOWLEDGEMENT

We thank ORTN BRIN for the financial support for this research. Also, thank Dr. Abu Khalid Rivai as the head of PRTDRAN for administrative permission and assistance in facilitating research activities.

## REFERENCES

- [1]. B. J. Park, J. J. Choi, J. S. Choe, O. Gileva, C. Ha, A. Iltis, E. J. Jeon, D. Y. Kim, K.W. Kim, S. K. Kim, Y. D. Kim, Y. J. Ko, C. H. Lee, H. S. Lee, I. S. Lee, M. H. Lee, S. H. Lee, S. J. Ra, J. K. Son, and K. A. Shin. "Development of ultra-pure NaI(Tl) detectors for the COSINE-200 experiment." *Eur. Phys. J.C.*, vol. 80, no. 814, 2020.
- [2]. I. Singh, B. Singh, B. S. Sandhu, and A. D. Sabharwal. "Comparative study for intermediate crystal size of NaI(Tl) scintillation detector." *Rev. Sci. Instrum.*, vol. 91, p. 073105, 2020.
- [3]. X. Wu, P. Li, X. Wei, and J. Liu. "Review: All-inorganic perovskite single crystals for optoelectronic detection." *Crystals*, vol. 12, no. 6, p. 792, 2022.
- [4]. R. Kubrin. "Nanophosphor coatings: Technology and applications, opportunities and challenge." *Powder and Particle Journal*, no. 31, pp. 22–52, 2014.

- [5]. B.D. Milbrath, A.J. Peurrung, M. Bliss, and W.J. Weber. "Radiation detector materials: An overview." *J. Mater. Res.*, vol. 23, no. 10, pp. 2561–2581, 2008.
- [6]. A. Dorokhina, R. Ishihara, H. Kominami, V. Bakhmetyev, M. Sychoy, T. Aoki, and H. Morii. "Solvothermal synthesis of LaF<sub>3</sub>:Ce nanoparticles for use in medicine: Luminescence, morphology and surface properties." *Ceramics*, vol. 6, no. 1, pp. 492–503, 2023.
- [7]. Y. Wang, Y. Wang, C. Huang, T. Chen, and J. Wu. "Ultra-weak chemiluminescence enhanced by cerium-doped LaF<sub>3</sub> nanoparticles: A potential nitrite analysis method." *Front. Chem.*, vol. 8, no. 639, 2020.
- [8]. A. T. Singh, M. M. Khandpekar, and S. G. Gaurkhede. "Enhanced luminescence of L-Alanine capped LaF<sub>3</sub>:Ce nanoparticles useful in biological labeling." *Journal of Nano Research*, vol. 32, pp. 81–92, 2015.
- [9]. L. Zhang, W. Li, X. Hu, Y. Peng, J. Hu, X. Kuang, L. Song, and Z. Chen. "Facile one-pot sonochemical synthesis of hydrophilic ultrasmall LaF<sub>3</sub>:Ce,Tb nanoparticles with green luminescence." *Progress in Natural Science: Materials International*, vol. 22, no. 5, pp. 488–492, 2012.
- [10]. S. G. Gaurkhede. "Synthesis and Studies Room Temperature Conductivity, Dielectric Analysis of LaF<sub>3</sub> Nanocrystals." *Nanosystems: Physics, Chemistry, Mathematics*, vol. 5, no. 6, pp. 843–848, 2014.
- [11]. A. T. Singha and M. M. Khandpekar. "Synthesis and structural studies of LaF<sub>3</sub>:Ce nanoparticles modified by tyrosine for bioimaging and biotagging applications." *Materials Today: Proceedings*, vol. 3, no. 10, pp. 4260–4265, 2016.
- [12]. F. Yang. "Synthesis, Characterization and Fluorescence Performance of LaF<sub>3</sub>:Ce<sup>3+</sup> Nanocrystals." Thesis, The University of New Mexico, New Mexico, 2009.
- [13]. T. Rogers, C. Han, B. Wagner, J. Nadler, and Z. Kang. "Synthesis of luminescent nanoparticle embedded polymer nanocomposites for scintillation applications." *Mater. Res. Soc. Symp. Proc.*, vol. 1312, 2011.
- [14]. A. Jain, C. Blum, and V. Subramaniam. "Fluorescence lifetime spectroscopy and imaging of visible fluorescent proteins." in *Chapter 4: Advances in Biomedical Engineering*, Elsevier B.V., 2009, pp. 147–176.
- [15]. D. Chateigner, X. Chen, M. Ciriotti, R. T. Downs, S. Gražulis, W. Kaminsky, A. L. Bail, L. Lutterotti, Y. Matsushita, A. Merkys, P. Moeck, P. M. Rust, M. Q. Olozabal, H. Rajan, A. Vaitkus, and A. F.T. Yokochi. *CIF File No.1538557*, Crystallography Open Database. Available: <http://www.crystallography.net/cod/>
- [16]. K. Schlyter. "On the crystal structure of fluorides of the tysonite LaF<sub>3</sub> type." *Arkiv for Kemi*, vol. 5, pp.73–82, 1952.
- [17]. D. Chateigner, X. Chen, M. Ciriotti, R. T. Downs, S. Gražulis, W. Kaminsky, A. L. Bail, L. Lutterotti, Y. Matsushita, A. Merkys, P. Moeck, P. M. Rust, M. Q. Olozabal, H. Rajan, A. Vaitkus, and A. F.T. Yokochi *CIF File No.1000041*, Crystallography Open Database. Available: <http://www.crystallography.net/cod/>
- [18]. D. Chateigner, X. Chen, M. Ciriotti, R. T. Downs, S. Gražulis, W. Kaminsky, A. L. Bail, L. Lutterotti, Y. Matsushita, A. Merkys, P. Moeck, P. M. Rust, M. Q. Olozabal, H. Rajan, A. Vaitkus, and A. F.T. Yokochi. *CIF File No.1528322*, Crystallography Open Database, Available: <http://www.crystallography.net/cod/>
- [19]. S. Ryufuku, Y. Tomota, Y. Shiota, T. Shiratori, H. Suzuki, and A. Moriai. "Neutron diffraction profile analysis to determine dislocation density and grain size for drawn steel wires." *Materials Science Forum*, vol. 539–543, pp. 2281–2286, 2007.
- [20]. K. N. Shinde, S.J. Dhoble, H.C. Swart, and K. Park. "Chapter 2: Basic mechanisms of photoluminescence" in *Phosphate Phosphors for Solid-State Lighting*, Springer Series in Materials Science 174, pp. 41–59, 2012.
- [21]. J. R. Albani, *Principles and Applications of Fluorescence Spectroscopy*, Blackwell Publishing, pp. 96, 2007.
- [22]. V. Retivov, V. Dubov, I. Komendo, P. Karpyuk, D. Kuznetsova, P. Sokolov, Y. Talochka, and M. Korzhik. "Compositionally disordered crystalline compounds for next generation of radiation detectors." *Nanomaterials*, vol. 12, no. 23, pp. 4295, 2022.
- [23]. N. Shrivastava, L. U. Khan, J. M. Vargas, C. Ospina, J. A. Q. Coaquira, G. Zoppellaro, H. F. Brito, Y. Javed, D. K. Shukla, M. C. F. C. Felinto, and S. K. Sharma. "Efficient multicolor tunability of ultrasmall ternary doped LaF<sub>3</sub> nanoparticles: energy conversion and magnetic behavior." *Phys. Chem. Chem. Phys.*, vol. 19, no. 28, pp. 18660–18670, 2017.

